Propagation of femtosecond optical pulses through uncoated and metal-coated near-field fiber probes

Roland Müller[a] and Christoph Lienau
Max-Born-Institut für Nichtlineare Optik und Kurzzeitspektroskopie, Max-Born-Str. 2A, D-12489 Berlin, Germany

(Received 14 December 1999; accepted for publication 12 April 2000)

The spatiotemporal evolution of a 10-femtosecond light pulse ($\lambda=805$ nm) propagating through uncoated and metal-coated near-field fiber probes is analyzed theoretically within a two-dimensional model for *s* and *p* polarization of the incident field. Internal reflection inside uncoated fiber probes (cone angle of 28°) results in an efficient guiding towards the fiber tip and a diffraction-limited spatial resolution of about 260 nm$\approx\lambda/3$ in case of *s* polarization. While the transmission through uncoated fiber probes has negligible effects on the temporal and spectral pulse profile, strong modifications are observed for metal-coated aperture probes. The wavelength-dependent aperture transmission gives rise to a pronounced blueshift and spectral narrowing of the transmitted pulses. © *2000 American Institute of Physics.* [S0003-6951(00)05023-3]

The combination of near-field microscopy and femtosecond spectroscopy attracts considerable interest as it opens up a new direction for studying ultrafast spatiotemporal dynamics of optical excitations in molecular and semiconductor nanostructures on nanometer length scales.[1,2] This gives direct access to, e.g., diffusive[3,4] and ballistic[5] carrier transport in semiconductors or to nonequilibrium dynamics[2] in single nanostructures. In such experiments, femtosecond temporal resolution is in general obtained by probing optical nonlinearities using pump-and-probe techniques. Subwavelength spatial resolution is achieved by transmitting femtosecond pump and/or probe pulses through either metal-coated or uncoated near-field fiber probes.

The transmission properties of such aperture probes for time-independent monochromatic light fields have been theoretically studied in great detail over recent years.[6] A number of theoretical methods have been developed and implemented for solving the vector Maxwell equations in the complex three-dimensional geometries that are typical for realistic near-field probes.[7] Among them are the Green's tensor technique,[8] the multiple–multipole technique[9] and finite-difference time domain methods (FDTD).[10] For uncoated fiber probes, near-field resolution down to $\lambda/4$ was only found in a special internal reflection geometry with polarization-resolved detection.[11] For metal-coated aperture probes, the studies show consistently the strong light localization in the near-field of the aperture as well as the pronounced wavelength, geometry, and polarization dependence of the transmission.[12,13] Yet, little is known about the effect of such probes on ultrashort light pulses.

In this letter, we present a theoretical study of the propagation of 10-fs light pulses through uncoated and metal-coated near-field fiber probes. Pronounced spectral shifts and temporal broadening effects are predicted in the near-field of metal-coated aperture probes.

Our simulations are based on a two-dimensional model assuming a trapezoidal geometry for the fiber taper in the y-z plane, Fig. 1(a). At the entrance of the taper, $z=2$ μm, the fiber is surrounded by a thin metal film to restrict the incident field to the taper dimension. The electric field of the incident light pulse is polarized either along the x axis, corresponding to *s* polarization with three nonzero electric and magnetic field components only, viz. E_x, H_y, and H_z, or along the y axis corresponding to *p* polarization with nonzero E_y, E_z, and H_x components only.[14] In the case of *s* polarization Maxwell's curl equations, governing light propagation, may be cast in the following form:

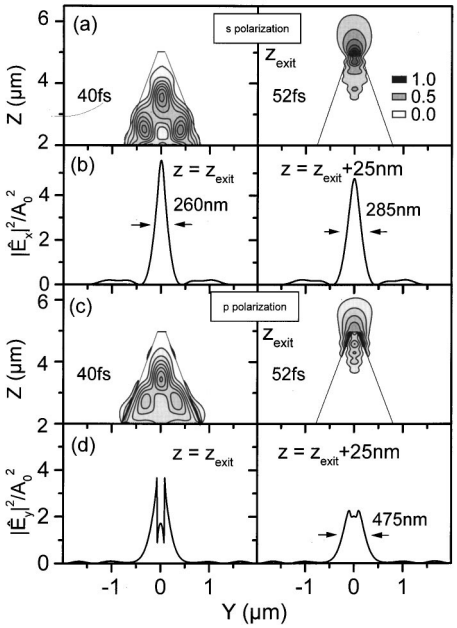

FIG. 1. Spatiotemporal evolution of a 10-fs optical pulse propagating through an uncoated near-field fiber probe. The peak intensity of the pulse arrives at the taper entrance ($z=2$ μm) at a time $t=36.7$ fs. (a) *s* polarization: Normalized energy density $|\hat{E}_x|^2/A_0^2$ at $t=40$ fs (left) and $t=52$ fs (right, maximum value of $|\hat{E}_x|^2$ at fiber exit). The linear gray scale is proportional to $|\hat{E}_x|^2/A_0^2$. (b) *s* polarization: Cross sections through Fig. 1(a) (right) at two different z coordinates: at the taper exit z_{exit} (left) and at $z_{exit}+25$ nm (right). (c) and (d) same as (a) and (b), respectively, but for *p* polarization.

[a]Author to whom all correspondence should be addressed; electronic mail: rmueller@mbi-berlin.de

$$\mu_0 \frac{\partial H_y}{\partial t} = -\frac{\partial E_x}{\partial z}$$

$$\mu_0 \frac{\partial H_z}{\partial t} = \frac{\partial E_x}{\partial y} \tag{1}$$

$$\epsilon\epsilon_0 \frac{\partial E_x}{\partial t} = \frac{\partial H_z}{\partial y} - \frac{\partial H_y}{\partial z},$$

where ϵ_0 and μ_0 are the permittivity and magnetic permeability of free space, respectively. The optical properties of matter (no absorption losses) are described by a real, frequency-independent dielectric function $\epsilon=\epsilon(y,z)$. Dispersion effects are neglected since the light paths in the media are only a few microns in length. Glass near-field fiber probes ($\epsilon=2.25$ inside the taper) both with and without metal coating are investigated. The metal coating is assumed to be a perfect conductor. A corresponding set of Maxwell's equations for p polarization is obtained from Eq. (1) if we make the following changes $E\rightarrow H$, $H\rightarrow -E$, $\epsilon_0\epsilon\rightarrow\mu_0$, and $\mu_0\rightarrow\epsilon_0\epsilon$.

As a numerical technique, we employ a two-dimensional FDTD code. The space grid is composed of 320 (in y)$\times$640 (in z) or 160$\times$320 cells with space increments $\Delta y=\Delta z=12.5$ nm (glass tip) or $\Delta y=\Delta z=6.25$ nm (metal-coated tip). The time increments are about 0.030 fs or 0.015 fs, respectively.

We consider a 10-fs Gaussian input pulse of plane-wave structure in the x-y plane that propagates along the z direction, $E_{x,\mathrm{in}}(t,z)$ (s polarization). The pulse spectrum is centered at a vacuum wavelength $\lambda_0=805$ nm. In front of the taper, $z<2$ μm, $E_{x,\mathrm{in}}=\hat{E}_{x,\mathrm{in}}+\hat{E}^*_{x,\mathrm{in}}$ with $\hat{E}_{x,\mathrm{in}}=A_0\exp(-2\ln 2\{[(t-t_0)-z/c]/\tau_0\}^2+\mathrm{i}ck_0[(t-t_0)-z/c])$. A_0 is one half of the field amplitude, $\tau_0=10$ fs and $k_0=2\pi/\lambda_0$. At $t=t_0=30$ fs the peak intensity of the pulse is centered at $z=0$. $\hat{E}^*_{x,\mathrm{in}}$ denotes the complex conjugate of $\hat{E}_{x,\mathrm{in}}$. Corresponding expressions hold for $H_{y,\mathrm{in}}$, while $H_{z,\mathrm{in}}=0$. The instantaneous electric energy density of the input pulse at space–time (z,t) is given by $\epsilon_0 E^2_{x,\mathrm{in}}$, including a high-frequency modulation factor $\cos^2\{ck_0[(t-t_0)-z/c]\}$. The corresponding envelope for the electric energy density is described by $4\epsilon_0|\hat{E}_{x,\mathrm{in}}|^2$. The maximum value of $|\hat{E}_{x,\mathrm{in}}|^2$ is given by A_0^2. The electric field $E_x(t,y,z)=\hat{E}_x+\hat{E}^*_x$ in the presence of dielectrica follows from Eq. (1) which, as a linear system with real coefficients, transforms $\hat{E}_{x,\mathrm{in}}$ in $\hat{E}_x$. For p polarization, the input pulse fields $E_{y,\mathrm{in}}$, $H_{x,\mathrm{in}}$ have the same (z,t) dependence as the respective s-polarized fields ($E_{x,\mathrm{in}}$,$H_{y,\mathrm{in}}$), while $E_{z,\mathrm{in}}=0$.

Figure 1(a) shows the spatial distribution of $|\hat{E}_x|^2$ (s polarization) in the y-z plane at times $t=40$ fs and $t=52$ fs (maximum value of $|\hat{E}_x|^2$ at fiber exit) for an uncoated probe with a cone angle of $\alpha=28°$. The maximum value of $|\hat{E}_{x,\mathrm{in}}|^2$ of the incident pulse arrives at $t=36.7$ fs at the entrance of the fiber tip ($z=2$ μm). Internal reflection inside the taper results in an efficient guiding towards the fiber tip. Cross sections through Fig. 1(a) (right) at fixed z values (i) $z=z_{\mathrm{exit}}$ and (ii) $z=z_{\mathrm{exit}}+25$ nm are shown in Fig. 1(b), representing the transmitted pulse shape along y at the exit of the tip (left) and 25 nm behind it (right). The internal guiding results in a spot size at the fiber exit of about 260 nm or $\lambda_{\mathrm{vacuum}}/3.1$. The low intensity wings seen on the left and right of the central peak are due to light that is escaping from the taper several hundred nanometer above its exit. The areas of the two peaks in Fig. 1(b), $\int|\hat{E}_x|^2dy$, differ only slightly from each other, which indicates that the transmitted light consists mainly of propagating waves resulting in a spatial resolution close to the diffraction limit. The transmission coefficient of such a probe is close to unity.

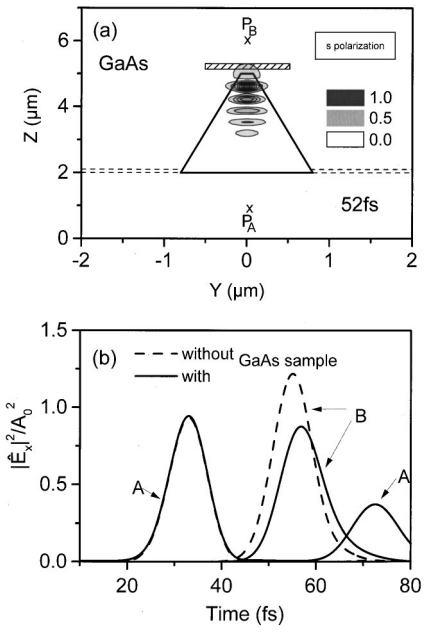

FIG. 2. (a) Effect of a semiconductor medium ($\epsilon=12.25$, no absorption) on the pulse propagation (s polarization). Shown is $|\hat{E}_x|^2/A_0^2$ for $t=52$ fs on a linear gray scale. Local reflection off the sample surfaces gives rise to pronounced interference patterns. (b) Temporal variation of $|\hat{E}_x(y,z,t)|^2/A_0^2$ at positions $P_A(y=0,z=1\ \mu\mathrm{m})$ and $P_B(y=0,z=6\ \mu\mathrm{m})$.

Corresponding results for p polarization are presented in Figs. 1(c) and 1(d). A comparison to Figs. 1(a) and 1(b) shows that waveguiding by the taper is more efficient for s than for p polarization resulting in a higher spatial resolution for s-polarized pulses at the fiber exit.

The calculated spatial resolution for s polarization as well as the observation of weak wings on both sides of the central peak [Fig. 1(b)] are in quantitative agreement with experimental results that have been obtained with similar probes.[2] This suggests that the two-dimensional simulations for s-polarized input fields are of particular relevance for comparison to realistic three-dimensional fiber probes which support preferentially the fundamental HE_{11} mode. For uncoated probes, we find, for both input polarizations, no noticeable change in the spectral or temporal shape of the transmitted pulses.

When a 100 nm thick GaAs layer ($\epsilon=12.25$; no absorption) is brought close to the fiber exit [Fig. 2(a)], we observe noticeable interference patterns inside the fiber due to the light field that is reflected from the sample. The pronounced contrast of the interference patterns is due to a high reflectivity of the semiconductor sample for the light field ($r\approx0.53$). This shows that such a probe is a highly efficient collector of the **locally** reflected field. This is supported by curves A and B [Fig. 2(b)] showing the temporal dependence of $|\hat{E}_x|^2/A_0^2$ at two different positions P_A and P_B outside the near-field region of the taper [Fig. 2(a)]. The difference in

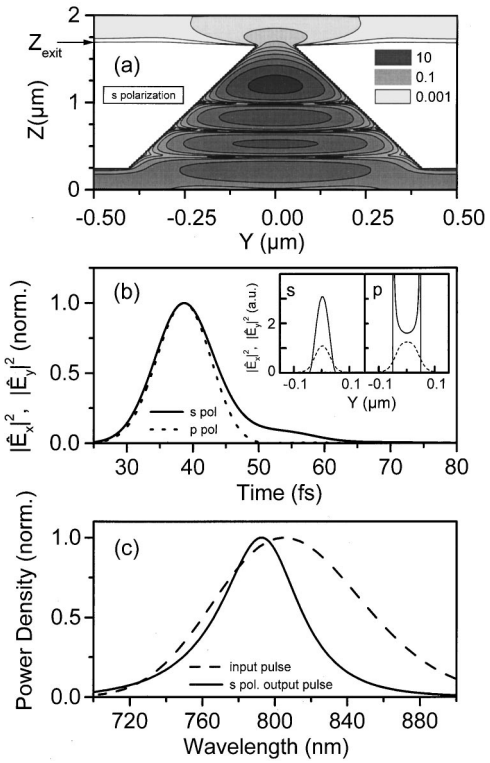

FIG. 3. Spatiotemporal evolution of a 10-fs light pulse propagating through a metal-coated fiber probe of 100 nm aperture diameter. The peak intensity of the pulse arrives at the taper entrance ($z=0.25$ μm) at a time $t=30.8$ fs. (a) Spatial distribution for s polarization of $|\hat{E}_x|^2/A_0^2$ at $t=38.7$ fs (maximum value of $|\hat{E}_x|^2$ at fiber exit) on a logarithmic gray scale. (b) Temporal variation of $|\hat{E}_x(y=0,z_{\text{exit}}+25\text{ nm},t)|^2$ (s polarization) and $|\hat{E}_y(y=0,z_{\text{exit}}+25\text{ nm},t)|^2$ (p polarization), normalized to their respective peak values at $t=38.7$ fs. The ratio of the absolute peak values is $|\hat{E}_{x,\text{peak}}|^2/|\hat{E}_{y,\text{peak}}|^2\approx 2\times 10^{-5}$. Inset: $|\hat{E}_x(y,z,t=38.7\text{ fs})|^2$ (s polarization, left) and $|\hat{E}_y(y,z,t=38.7\text{ fs})|^2$ (p polarization, right) at $z=z_{\text{exit}}$ (solid lines) and $z=z_{\text{exit}}+25$ nm (dashed). (c) Spectral power density of the Gaussian input pulse (dashed line) and of the s-polarized transmitted pulse at $z=z_{\text{exit}}+25$ nm (solid line).

pulse energies of the transmitted pulse in the absence (dashed curve B) and presence (solid curve B) of the semiconductor sample is close to the energy of the reflected pulse in the presence of the semiconductor (solid curve A, $t>60$ fs), evidencing the high collection efficiency.

Strongly different effects are observed for near-field probes with a perfectly conducting metal coating. Here, the spatial resolution directly behind the aperture is defined by the aperture diameter. Figure 3(a) shows $|\hat{E}_x|^2/A_0^2$ (s polarization) inside and behind a metal-clad fiber with a 100 nm aperture diameter. Inside the fiber, pronounced interference patterns are formed between the incoming and internally reflected field, making such probes rather insensitive to small local reflections from sample surfaces. For s polarization, the intensity of the transmitted pulse is strongly reduced by more than three orders of magnitude. The temporal shape of the transmitted s-polarized pulse at a distance of 25 nm from the fiber exit indicates a significant deviation from that of the 10-fs Gaussian [Fig. 3(b)]. The inset shows the lateral intensity profiles of the transmitted pulses for s (left) and p (right) polarization at the fiber exit (solid curves) and 25 nm behind it (dashed). The large differences between the areas of the two s- or p-polarized pulses indicate the dominant contribution of evanescent waves, in contrast to uncoated probes. Figure 3(c) shows a strong narrowing of the transmitted pulse spectrum (s polarization) by about 40% and a pronounced blueshift by more than 15 nm (solid curve) compared with the spectrum of the incident Gaussian pulse (dashed) whereas the spectrum of a p-polarized pulse is very similar to that of the Gaussian (not shown). The transmission coefficient through a two-dimensional slit is close to unity[15] for p polarization and therefore only minor effects of the transmission on the temporal pulse profile [Fig. 3(b), dashed curve] and pulse spectrum are expected and found.

The pronounced change of the transmitted pulse spectrum and temporal profile for s-polarized incident fields may be attributed to the wavelength dependent transmission efficiency of metal-coated probes that strongly favor the transmission of shorter wavelengths. For idealized geometries, such as an infinite slit in a very thin perfect metallic screen[15] analytic solutions for the transmission T are known. For a plane wave of wave number k and an electric vector oscillating parallel to the edges of the slit T is proportional to $(ka)^3$ if $ka\ll 1$. This solution predicts, in fact, a blueshift of the transmitted s-polarized pulse spectrum, while the width of the spectrum is only slightly changed. However, the analytical solution does not account for the pronounced spectral narrowing and the reduction in power density in the blue part of the pulse spectrum that are indicated by our simulations. We attribute these effects to the complex geometry of the tapered aperture probe that results in transmission properties for ultrashort pulses that are distinctly different from those expected for an idealized geometry.

In conclusion, we have investigated theoretically the propagation of 10-fs optical pulses through near-field fiber probes. For uncoated fiber probes, a spatial resolution down to $\lambda/3$ and transmission and collection efficiencies close to unity are predicted. Metal-coated probes allow us to further improve the spatial resolution but their complex wavelength-dependent transmission properties affect both the spectral and temporal profiles of ultrashort light pulses.

[1] B. A. Nechay, U. Siegner, F. Morier-Genoud, A. Schertel, and U. Keller, Appl. Phys. Lett. **74**, 61 (1999).
[2] T. Guenther, V. Emiliani, F. Intonti, C. Lienau, T. Elsaesser, and K. H. Ploog, Appl. Phys. Lett. **75**, 3500 (1999).
[3] V. Emiliani, T. Guenther, C. Lienau, R. Nötzel, and K. H. Ploog, Phys. Rev. B **61**, R10583 (2000).
[4] M. Achermann, B. A. Nechay, F. Morier-Genoud, A. Schertel, U. Siegner, and U. Keller, Phys. Rev. B **60**, 2101 (1999).
[5] B. Hanewinkel, A. Knorr, P. Thomas, and S. W. Koch, Phys. Rev. B **60**, 8975 (1999).
[6] For a recent overview, the reader is referred to J. Microsc. **194**, 229 (1999).
[7] C. Girard and A. Dereux, Rep. Prog. Phys. **59**, 657 (1996).
[8] O. J. F. Martin, C. Girard, and A. Dereux, Phys. Rev. Lett. **74**, 526 (1995).
[9] Ch. Hafner and L. H. Bomholdt, *The 3d Electrodynamic Wave Simulator* (Wiley, Chichester, England, 1993).
[10] K. S. Kunz and R. J. Luebbers, *The Finite Difference Time Domain Method for Electromagnetics* (CRC Press, Boca Raton, FL, 1993).
[11] G. von Freymann, T. Schimmel, M. Wegener, B. Hanewinkel, A. Knorr, and S. W. Koch, Appl. Phys. Lett. **73**, 1170 (1998).
[12] L. Novotny, D. W. Pohl, and B. Hecht, Ultramicroscopy **61**, 1 (1995).
[13] A. Chavez-Pirson and S. T. Chu, Appl. Phys. Lett. **74**, 1507 (1999).
[14] J. L. Kann, T. D. Milster, F. F. Froehlich, R. W. Ziolkowski, and J. B. Judkins, J. Opt. Soc. Am. A **12**, 501 (1995).
[15] C. J. Bouwkamp, Rep. Prog. Phys. **17**, 35 (1954).